Groundwater sapping as the cause of irreversible desertification of Hunshandake Sandy Lands, Inner Mongolia, northern China

- Supplementary Information (SI) Appendix –

Xiaoping Yang[1], Louis A. Scuderi[1], Xulong Wang, Louis J. Scuderi, Deguo Zhang, Hongwei Li, Steven Forman, Qinghai Xu, Ruichang Wang, Weiwen Huang, Shixia Yang

[1]Corresponding authors. E-mails: xpyang@mail.igcas.ac.cn; xpyang@263.net.cn (X.Y.) or tree@unm.edu; cirque1@gmail.com (L.A.S.)

This PDF file includes:

1. Supplementary Figures: S1-S6
2. Supplementary Tables: S1-S3
3. Additional Details of Methods

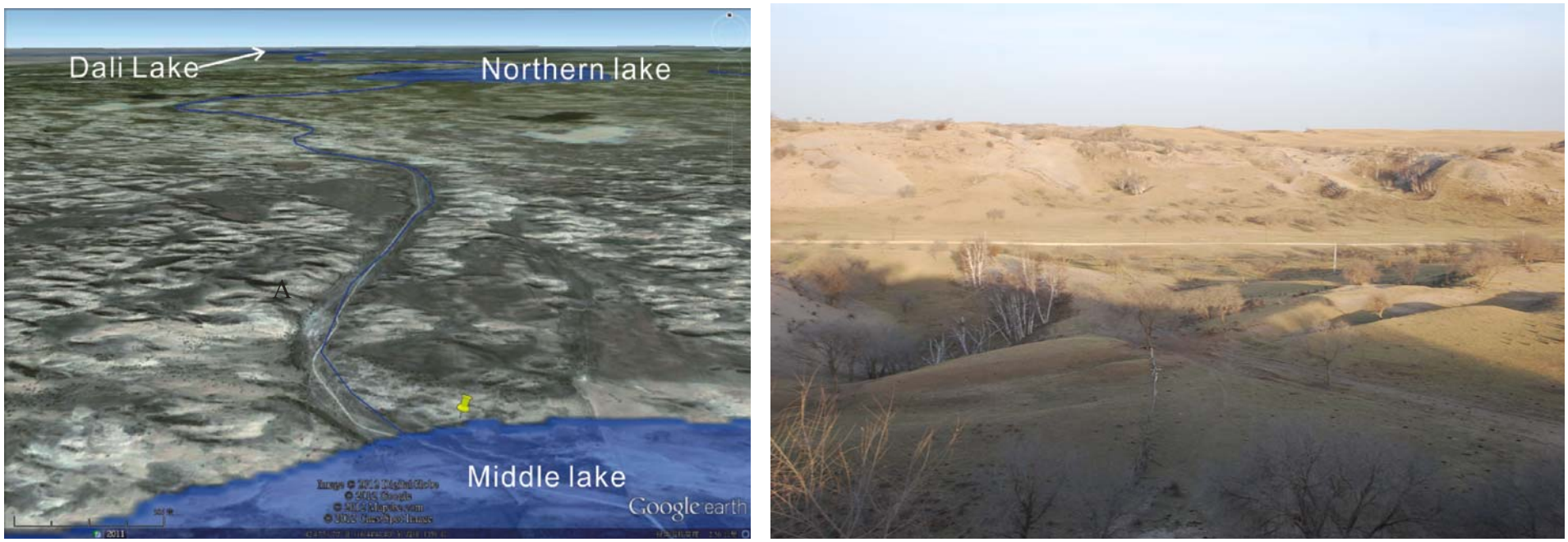

Fig. S1. Left: Google Earth image of the terrace and the linear channel linking the middle (Lake B) and lower (Lake C) lakes (for locations see Fig. 2 in the main text). **Right:** Photo of the channel taken at site A (see left for location), viewing towards NE.

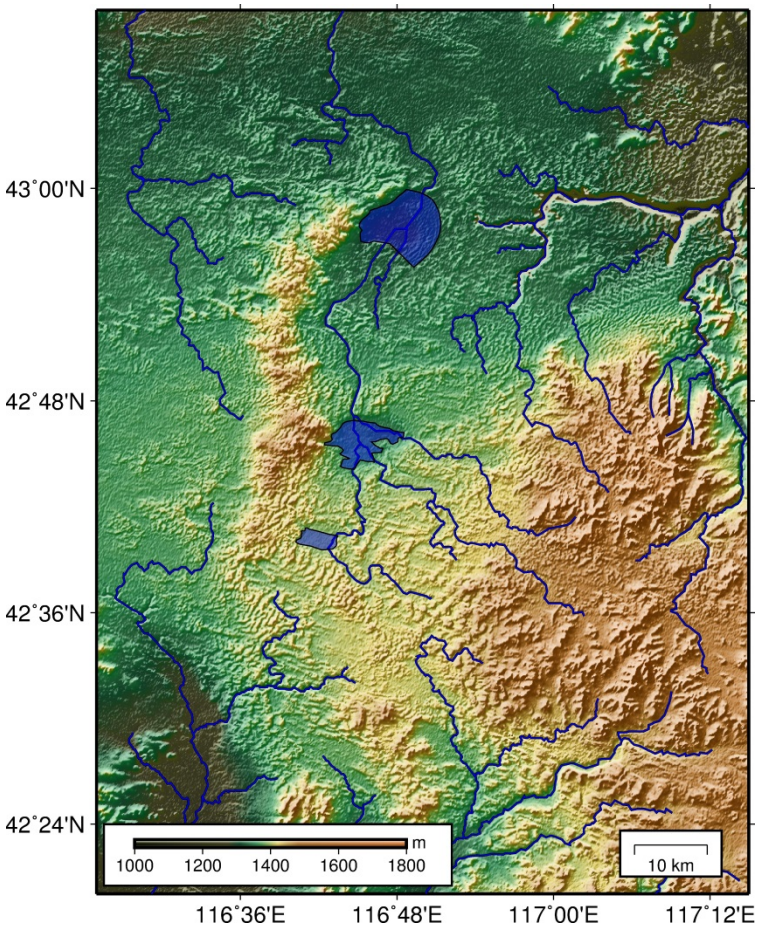

Fig. S2. River nets identified from SRTM elevation data, showing that the lakes were recharged by streams with head waters to the southeast prior to capture by the eastward flowing Xilamulun River via ground water sapping.

Fig. S3. Laminated lacustrine sediments in section H (for location of the section see Fig. 1 in the main text), showing that the water in the central areas of the lake was relatively deep.

Fig. S4. Terraces above the main channel of the Xilamulun River formed by flows from headwater sapping drainage post-4200 years ago.

Fig. S5. Examples of ceramics found in section I, that were pieces of casseroles (left) used for cooking by Hongshan people. Stone tools collected in sections M and F (right), suggesting long-term residential sites of the Hongshan culture (1, 2, Borers; 3, 4, Blades; 5, Burin; 6, 7, 10, 11, Flakes; 8, 9, Scrapers. For locations of the sections see Fig. 1 in the main text).

Fig. S6. Changing images of the dragon in Chinese culture. **Left:** Coiled trout form of the first jade dragon of China. The earliest examples, all found within 150 km of our study area, have been linked to Hongshan Culture (4500 to 2700 BC). The pig head/snout form has been associated with pig domestication within the Hongshan culture. **Right:** Subsequent dragons are usually depicted with scales and feet.

Table S1. Diatoms identified in the lacustrine sediments (for location of the sections see Fig. 1 in the main text) in the Hunshandake Sandy Lands.

Diatoms	C	D	F	I_a	I_b (Second Sample from I
Pediastrum	*	*		*	*
Concentricystes	+	+			
Cyclotella	*	*		+	
Stephanodiscus	*	*		+	
Melosira	+				
Phacus			+		
Cymbella	+				
Navicula	+				
Westella				+	
Nematode				+	
Notes	Particularly abundant	Particularly abundant			

+ present， * abundant

Note: Field identification of lacustrine sediments is confirmed by the occurrence of diatoms in all sections sampled. The types of diatoms recorded point to fresh water conditions (For digital photos of the frequently occurring taxa please see next page).

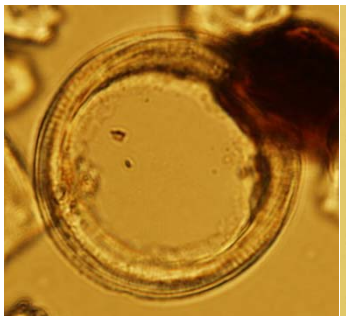

Stephanodiscus

Cymbella

Navicula

Concentricystes

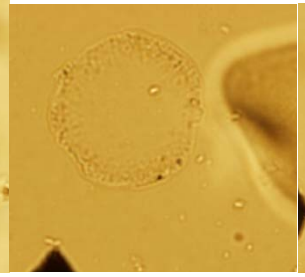

Cyclotella

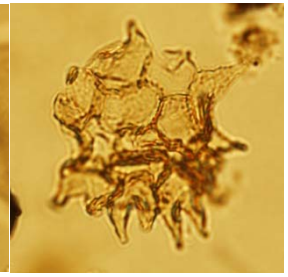

Pediastrum

Microcystis

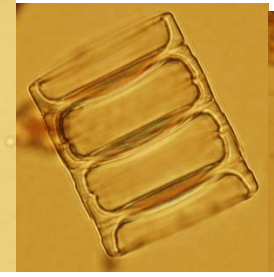

Melosira

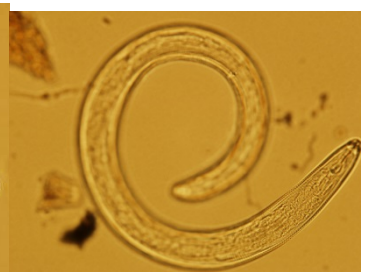

Nematode

Table S2. Neolithic stone tools and ceramics found along the shorelines of the former lakes (for localities see Figs. 1 and 2 in the main text)

	Lake C			Lake B	Lake A	Section P
Lithic artifacts	Sections C, D	Section I	Section F			
Borers				7		
Burins				1		
Scrapers	4	2	1	5		1
Notches				2		
Arrowhead				2		
Flakes	5	1		39		
Blades			2	6	1	
Denticulates	1					
Cores	1			1		
Wastes	50	7		37		
Unidentified tools	8	46	37	294		
Total	69	56	40	394	1	1
Ceramics	91	43	35	35	23	24

Table S3. Water sample tritium content (for locations see Fig. 1 in the main text)

NO.	Depth（m）	N	E	Elevation (m a.s.l.)	Tritium content (TU）
1	60	42°58'1.6"	116°49'39.1"	1317	1.86
2	37	42°56'39.5"	116°45'33.1"	1321	18.7
3	6	42°40'34.3"	116°41'13.9"	1400	4.14
4	27	42°45'34.4"	116°45'38"	1362	9.97
5	7	42°45'36.4"	116°45'36.9"	1365	22.9
6	16	42°48'22.9"	116°44'52.1"	1352	19.6
7	30	42°51'1.2"	116°44'8.6"	1347	24.3

Additional Details of Methods

1. OSL Dating

Samples for Optically Stimulated Luminescence (OSL) dating were collected in stainless tubes (with an interior diameter of 4 cm and a length of 30 cm) hammered into freshly-cleaned section faces. The sample tubes were immediately sealed with opaque tape and well wrapped in the field and transported to the laboratories smoothly to have avoided any unwanted shaking. Sediment from both ends of the sample tubes was excluded from equivalent dose (*De*) estimation, and it was used for radioisotope measurements to obtain the environmental dose rate.

1.1. ED (D_e) determination

Equivalent dose (D_e) value is determined by Single-aliquot Regenerative-dose (SAR) protocol (1) in both Xi'An (Table M_1a) and Chicago (Table M_1b) laboratories. For the different experimental instruments (e.g. Daybreak and Risø reader) were used, the experimental parameters have been determined independently by both laboratories to have satisfied the criterions (e.g. preheating plateau, repeated and recuperation ratio, and also dose recovery results) (1). The data analysis of D_e determination was treated with the recently updated method by Wang et al. (2) in Xi'an laboratory, and the Chicago Laboratory followed methodological approaches of Murray and Wintle (1), Galbraith et al. (3) and Galbraith and Roberts (4). More details are as follows.

Table M_1

(a) SAR protocol used in Xian

Step	Treatment	Observed
1	Give regenerative dose (RD)	
2	Preheating at 260°C for 10 s	
3	IR stimulation at 125°C for 200 s	
4	Blue stimulation at 125°C for 200 s	L_i
5	Give test dose, 5 Gy	
6	Preheating at 220°C for 10 s	
7	IR stimulation at 125°C for 200 s	
8	Blue stimulation at 125°C for 200 s	T_i
9	Repeat Steps 1-8 for different RD	

(b) SAR protocol used in Chicago

Step	Treatment
1	Natural dose or give beta dose
2	Preheat 240^{o}C for 10 s
3	Stimulate with blue light (470 nm) for 40 s at 125^{o}C
4	Give beta test dose (6.6 Gray)
5	Preheat 220 ^{o}C for 10 s
6	Stimulate with blue light (470 nm) for 40s at 125^{o}C
7	Stimulate with blue light for 40 s at 280 ^{o}C
8	Return to step 1

1.1.1. Procedures applied in Xi'an

Pretreatments

Samples were pretreated with 30% HCl and 10% H_2O_2 to remove the carbonates and organic matter, respectively. Then the 90-125 μm fractions were sieved out and etched by HF (40%) for 45 minutes. The purity of the isolated quartz was checked by IR stimulation, and in the SAR dating protocol an additional IR bleaching (Step 3 and 7, Table M_1a) was also applied to further remove any signal from potential feldspar contamination.

ED determination and preheating plateau results

A Single-Aliquot Regenerative-dose (SAR) protocol was used to determine the Equivalent Dose (D_e) of the 90-125 μm quartzes (Table M_1a) (1). A test dose of 5 Gy was used (step 5) to measure the sensitivity Ti. The corrected OSL intensity for the

natural and regenerative dose was obtained as the slope of Li versus Ti as introduced by Wang et al. (2), rather than the Li/Ti ratio as used in the classic SAR protocol (1). Fig. M_1a presents the natural and its following test dose OSL decay curves for one aliquot, and Fig. M_1b shows the relationship between the natural or regenerated OSL (Li) and their following test dose OSL (Ti) responses for Sample IEE3791. The data for Li and Ti in Fig. M_1b were fitted by the equation Li = k*Ti+b, where k is the corrected OSL intensity for the SAR protocol, and b is the influence of OSL buildup in the SAR protocol as shown by Wang and Wintle (5). These corrected OSL intensities were used to construct the dose response curve and then a D_e was determined for each sample (Fig. M_1c). All results in Fig. M_1a, 1b and 1c were obtained with a preheating temperature of 260°C and 220°C for the natural (or regenerative) dose and test doses, respectively. Fig. M_1d presents all the results obtained using different preheating conditions as a preheating plateau test. The results confirm that 260°C is suitable for sample IEE3791, and this preheating condition was also used for all of the samples.

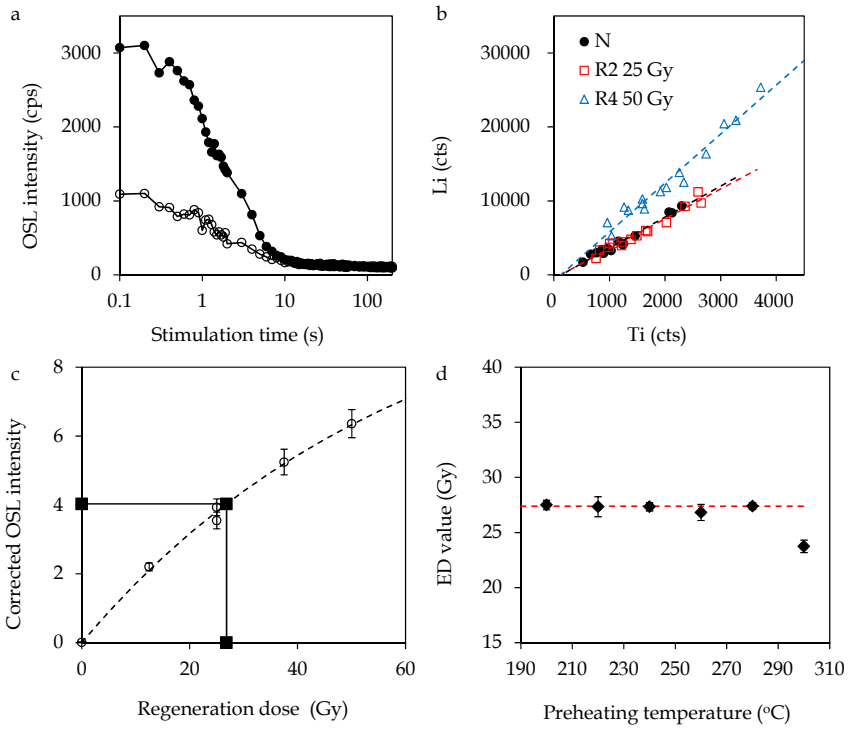

Fig. M_1. a) OSL decay curves for the natural dose and the following test dose of 5 Gy for sample IEE3791; b) relationship between natural (or regenerative) dose OSL and test dose OSL (first 5 s of decay curve); c) Dose response curve and D_e determination for OSL dating; d) D_e plateau for different preheating conditions.

Recovering the laboratory known dose

Aliquots of sample IEE3791 were bleached by a solar simulator (SOL 2) for 30 mins and then used to recover a laboratory known dose. Fig. M_2a presents the D_e results for both a natural and laboratory known dose of 25 Gy, using the classic SAR protocol, in which the corrected OSL intensity is the ratio of Li/Ti, rather than the slope of Li versus Ti. It can be seen that the De values for both natural and laboratory known doses show significant deviation as a function of the corrected OSL intensities of Li/Ti, and the D_e values range from 20 to 30 Gy (Fig. M_2b) when a laboratory known dose of 25 Gy was given. This is due to the intercept of b as shown in Fig. M_1b. However, the laboratory known dose of 25 Gy was well recovered, 24.7±0.2 Gy (last data point in Fig. M_2b), when using the slope of Li versus Ti as the corrected OSL intensity for D_e determination (2). Fig. M_2c presents the full procedure of the D_e determination

using the slope of Li versus Ti. Thus it is confirmed that the new SAR protocol using the slope of Li versus Ti as the corrected OSL intensity is appropriate for sample IEE3791; this protocol has been used for the D_e values for all samples (Table M_2a) dated in Xian.

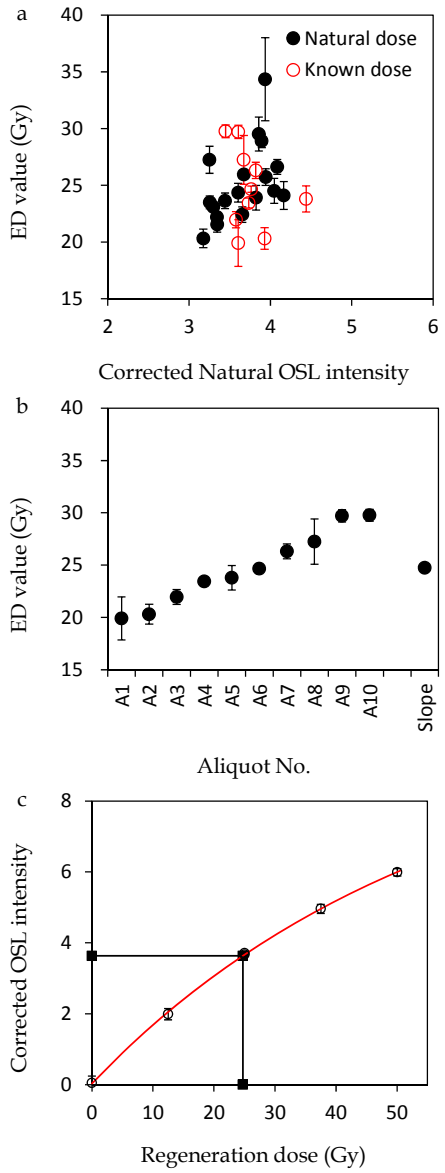

Fig. M_2. a) D_e values for natural or laboratory known dose (25 Gy) plotted against corrected OSL intensities; b) ED values for SAR protocol using L_x/T_x and also for slope of $L_x$versus T_x as corrected OSL intensities; c) dose recovery data set for laboratory known dose of 25 Gy.

1.1.2. Procedures applied in Chicago

Each aliquot contained approximately 100 to 200 quartz grains corresponding to a 1.5 to 2.0 millimeter circular diameter of grains adhered (with silicon) to a 1 cm diameter circular aluminum disc. Grain size of quartz was either 100-150 μm or 150-250 μm (Table M_2b). This aliquot size with the grain sizes was chosen to maximize light output for the natural with excitation; smaller aliquots often yielded insufficient emissions (< 400 photon counts/s). Sands analyzed were mineralogically mature with SiO_2 content of 80% to 89% and are predominantly (>80%) well-sorted quartz grains. The quartz fraction was isolated by density separations using the heavy liquid Na–polytungstate, and a 40-minute immersion in HF (40%) was applied to etch the outer ~10 μm of grains, which is affected by alpha radiation (6). Quartz grains were rinsed finally in HCl (10%) to remove any insoluble fluorides. The purity of quartz separate was evaluated by petrographic inspection and point counting of a representative aliquot. Samples that showed >1% of non-quartz minerals were retreated with HF and rechecked petrographically. The purity of quartz separates was tested by exposing aliquots to infrared excitation (1.08 watts from a laser diode at 845 ± 4 nm), which preferentially excites feldspar minerals. Samples measured showed weak emissions (<200 counts/second), at or close to background counts with infrared excitation, and ratio of emissions from blue to infrared excitation of >20, indicating a spectrally pure quartz extract (7).

A series of experiments was performed to evaluate the effect of preheating at 200, 220, 240, 260 and 280 °C for 10 seconds on thermal transfer of the natural and regenerative luminescence (L_x) as a dose recovery test (6.6 Gy) prior to the application of SAR dating protocols (1). These experiments showed modest preheat-based sensitivity changes with a full recovered dose (6.6 Gy) and well within one standard deviation at a preheat temperature of 240°C (Fig. M_3), which was used in all SAR analyses (Table M_1b). A "cut heat" at 220 °C for 10 s was applied prior to the measurement of the test dose (T_x) and a final heating at 280 °C for 40 s was applied to minimize carryover of luminescence to the succession of regenerative doses. The

luminescence signal of the natural, test dose and regenerative doses was fully dominated by the fast component with >90% diminution of signal after 2 seconds blue diode exposure (Fig. M_3).

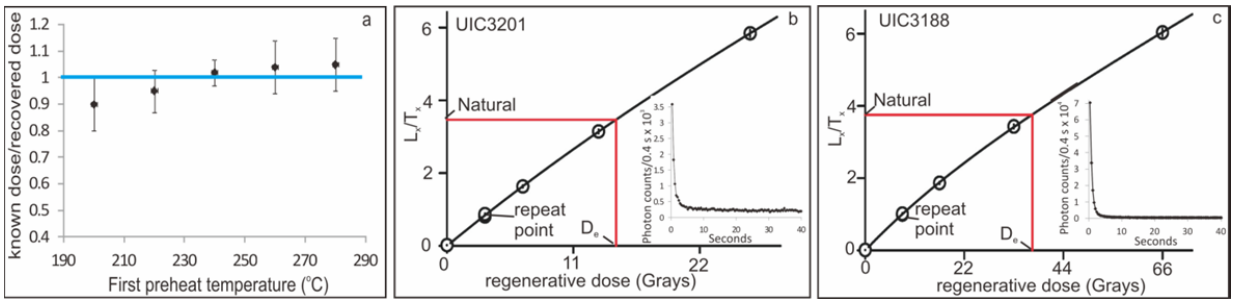

Fig. M_3. a) and b): Single aliquot regenerative dose plots, insert is representative shine down curve. c): Dose recovery data set for laboratory known dose of 6.6 Gy. Unity indicates agreement between known dose and recovered dose, preheat temperature used is 240 ^{o}C.

Calculation of equivalent dose by the single aliquot protocols was accomplished for 25 to 30 aliquots (Table M_2b). Regenerative dose curve was fit with a combined exponential and linear function (Fig. M_3). Equivalent dose errors where calculated assuming a measurement error of 1% and after 2000 Monte Carlo repeats. For most samples all or nearly all (28 or 29) aliquots were used for the final (*De*) distribution and age determination (Table M_2b; Fig. M_4). Equivalent dose (*De*) distributions were usually log normal and most (16/19) exhibited a narrow range of overdispersion values from 9% to 26% (Table M_2b; Fig. M_3). An overdispersion percentage of a *De* distribution is an estimate of the relative standard deviation from a central *De* value in context of a statistical estimate of errors (3, 4). A zero overdispersion percentage indicates high internal consistency in *De* values with 95% of the *De* values within 2σ errors. Overdispersion values ≤ 20% (at 2 sigma errors) are routinely assessed for quartz grains that are well solar reset, like eolian sands (8, 9) and this value is considered a threshold metric for calculation of a *De* value using the central age model of Galbraith and Roberts (4). Overdispersion values >20% indicate mixing or grains of

various ages or partial solar resetting of grains; the minimum age model (three parameters) may be an appropriate statistical treatment for such data and weights for the youngest *De* distribution (3, 4).

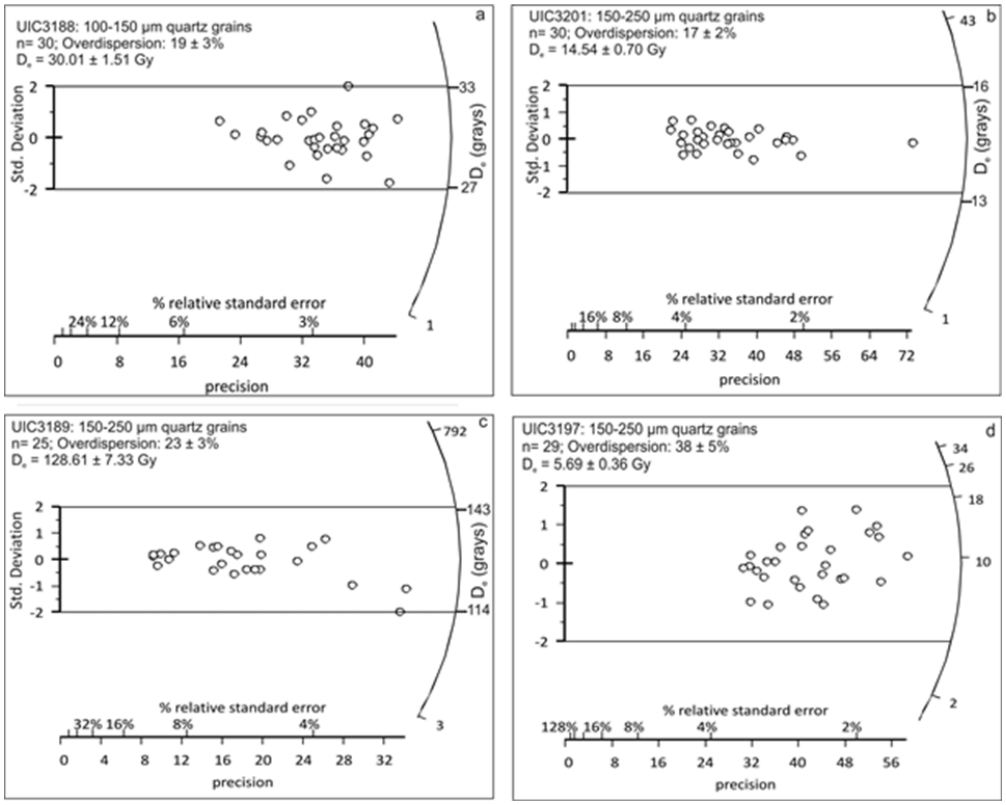

Fig. M_4. Radial plots of D_e values on small aliquot (2-mm plate of 150-250 µm or 100-150 µm quartz fraction grains)

1.2. Dose rate and OSL ages

A determination of the environmental dose rate is needed to render an OSL age, which is an estimate of the exposure of quartz grains to ionizing radiation from U and Th decay series, ^{40}K, and cosmic sources during the burial period. For the samples dated in Chicago, the U and Th content of the sediments, assuming secular equilibrium in the decay series, and ^{40}K, were determined by inductively coupled plasma-mass spectrometry (ICP-MS) analysed by Activation Laboratory LTD, Ontario, Canada. For

the samples dated in Xian, the concentrations of U and Th were measured using ICP-MS, while the potassium concentration was analyzed using ICP-OES in Changan University, Xian, China. A moisture content (by weight) of 10 ± 3 was used in dose rate calculations, which reflects the variability in field moisture conditions for the samples dated in Chicago, whereas an average moisture content of 10±5% was assumed for the samples dated in Xian. The beta and gamma doses were adjusted according to grain diameter to compensate for mass attenuation (10). A significant cosmic ray component between 0.02 and 0.24 mGy/yr was included in the estimated dose rate taking into account location, elevation and depth of strata samples (11). In the Laboratory in Xian the dose rate was calculated using the Dose4Win program supported by Prof. Andrzej Bluszcz (GADAM Centre of Excellence, Department of Radioisotopes, Institute of Physics, Silesian University of Technology, Gliwice, Poland), in which the dose rate conversion factors of Guérin et al. (12) were used.

Table M_2 OSL dating results

(a) Samples dated in Xi'an

Sample number	Laboratory number	Grain Size (μm)	Equivalent dose (Gray)	U (ppm)[a]	Th (ppm)[a]	K (%)[b]	Dose rate (Gray/ka)	OSL age (ka)
C-1	IEE3786	90-125	25.8 ± 0.9	0.69	1.50	2.06	2.38 ± 0.12	10.8 ± 0.7
C-2	IEE3787	90-125	24.5 ± 0.1	0.84	2.03	2.19	2.64 ± 0.12	9.3 ± 0.4
C-3	IEE3788	90-125	1.7 ± 0.1	0.68	1.53	2.45	2.71 ± 0.14	0.62 ± 0.05
C-4	IEE3789	90-125	1.9 ± 0.1	0.73	1.64	2.13	2.47 ± 0.12	0.78 ± 0.05
D-1	IEE3790	90-125	27.3 ± 1.0	0.73	1.51	2.36	2.65 ± 0.13	10.3 ± 0.6
D-2	IEE3791	90-125	26.8 ± 0.7	0.68	1.42	2.50	2.80 ± 0.14	9.6 ± 0.5
D-3	IEE3792	90-125	5.6 ± 0.1	0.82	1.71	2.23	2.66 ± 0.13	2.1 ± 0.1
E-1	IEE3793	90-125	28.2 ± 0.5	0.67	1.21	2.19	2.47 ± 0.12	11.4 ± 0.6
E-2	IEE3794	90-125	0.4 ± 0.1	0.69	1.43	1.89	1.78 ± 0.08	0.22 ± 0.03
F-2	IEE3795	90-125	17.8 ± 0.7	0.85	2.08	2.46	2.85 ± 0.14	6.3 ± 0.4
F-5	IEE3796	90-125	16.8 ± 0.3	0.88	2.21	2.33	2.80 ± 0.13	6.0 ± 0.3
I-0.6	IEE3797	90-125	9.6 ± 0.1	0.72	1.55	1.41	1.84 ± 0.08	5.2 ± 0.2
I-1.0	IEE3798	90-125	10.2 ± 0.3	0.66	1.24	1.45	1.81 ± 0.08	5.7 ± 0.3

[a] Analytical precision was better than 3% for the uranium and thorium concentrations.
[b] Analytical precision was better than 1% for the potassium concentrations.

(b) Samples dated in Chicago

Sample number	Laboratory number	Aliquots[a]	Grain Size (μm)	Equivalent dose (Gray)[b]	Over-dispersion (%)[d]	U (ppm)[e]	Th (ppm)[e]	K (%)[e]	Dose rate (mGray/yr)[f]	OSL age (yr)[g]
M-1	UIC3205	30/30	150-250	13.23 ± 0.62	17 ± 2	0.9 ± 0.1	2.2 ± 0.1	2.20 ± 0.02	2.39 ± 0.14	5440 ± 480
M-2	UIC3201	30/30	150-250	14.54 ± 0.70	17 ± 2	0.7 ± 0.1	2.0 ± 0.1	2.48 ± 0.02	2.58 ± 0.16	5630 ± 500
M-3	UIC3194	28/30	150-250	12.03 ± 0.72	23 ± 3	0.5 ±0.1	1.6 ± 0.1	2.17 ± 0.02	2.25 ± 0.13	5330 ± 510
P2-1	UIC3200	25/30	100-150	0.24 ± 0.04[c]	36 ± 5	0.8 ± 0.1	2.5 ± 0.1	2.28 ± 0.02	2.51 ± 0.15	95 ± 20
P2-2	UIC3198	25/30	150-250	0.42 ± 0.03	26 ± 4	0.7 ± 0.1	2.2 ± 0.1	2.28 ± 0.02	2.40 ± 0.14	175 ± 20
P2-3	UIC3199	27/30	150-250	3.55 ± 0.19	21 ± 3	0.8 ± 0.1	2.3 ± 0.1	2.15 ± 0.02	2.31 ± 0.14	1535 ± 140
P2-4	UIC3186	27/30	150-250	6.69 ± 0.38	24 ± 3	0.9 ± 0.1	2.8 ± 0.1	2.17 ± 0.02	2.37 ± 0.14	2820 ± 260
P2-5	UIC3206	30/30	100-150	9.68 ± 0.45	17 ± 2	0.8 ± 0.1	2.4 ± 0.1	2.08 ± 0.02	2.27 ± 0.14	4265 ± 380
P2-6	UIC3190	29/30	150-250	10.76 ± 0.56	20 ± 3	0.7 ± 0.1	2.2 ± 0.1	2.18 ± 0.02	2.27 ± 0.14	4740 ±430
P2-7	UIC3195	30/30	150-250	15.78 ± 0.75	19 ± 2	0.7 ± 0.1	2.4 ± 0.1	2.17 ± 0.02	2.28 ± 0.14	6930 ± 610
P2-8	UIC3207	30/30	100-150	13.89 ± 0.66	17 ± 2	0.6 ± 0.1	1.8 ± 0.1	2.28 ± 0.02	2.19 ± 0.13	6330 ± 565

[a]Aliquots used in equivalent dose calculations versus original aliquots measured.

[b]Equivalent dose calculated on a pure quartz fraction with about ~100-200 grains/aliquot (~2 mm plate area) and analyzed under blue-light excitation (470 ± 20 nm) by single aliquot regeneration protocols (1). The central age model (3) was used to calculated equivalent dose.

[c]Equivalent dose calculated using the minimum age model (3) because of elevated overdispersion values (>20% at 2 sigma limits).

[d]Values reflects precision beyond instrumental errors; values of ≤ 20% (at 2 sigma limits) indicate low dispersion in equivalent dose values and an unimodal distribution.

[e]U, Th and K content analyzed by inductively-coupled plasma-mass spectrometry analyzed by Activation Laboratory LTD, Ontario, Canada.

[f]A moisture content of 10 ± 3% for all samples.

[g]Systematic and random errors are included and reported errors are at one sigma; reference year for ages is AD 2010.

2. **Methods for identifying the diatoms:**

50 g of the sediments were sieved via 200 μm first and the particles > 200 μm was removed. The remaining samples were then put in a bath with distilled water and then wet sieved via 10 μm and particles < 10 μm were removed. Finally the samples were isolated via suspensions with the liquid density of 2.4. The suspensions were then diluted with distilled water and then the remains were finally isolated from water in a centrifuge tube. The genus of the diatoms was finally identified under a BX-51 Olympus light microscope at 400x magnification and more than 100 diatoms were counted for each sample.

3. Methods for tritium analysis:

Seven samples, 500 ml each, were collected from wells, 6 – 60 m deep, in the study area. 300 ml of water sample, added with 1 g $KMnO_4$, were distilled to remove any impurities. In order to increase the tritium concentration to an easily measurable level, electrolytic enrichment was applied (13, 14). 250 ml previously distilled sample with 2.5 g NaOH was then put to the electrolysis apparatus containing electrolytic cells with co-axial stainless steel electrodes. Electrolysis was carried out until the volume of electrolyte was reduced to 8 ml and all runs were performed at a temperature of 2 – 5 ^{o}C to prevent the loss of tritiated water molecules by evaporation. After electrolysis CO_2 was bubbled through the cell to neutralize the water because the medium in which the electrolysis took place earlier is alkaline. The water sample was separated from the electrolyte by distilling. The pretreated samples were measured by a low-level background liquid scintillation counter (Quantulus 1220-003) according to the manufacturer's guidelines. The error bar of the measurement should be < ±3%.

References

1. Murray AS, Wintle AG (2003) The single aliquot regenerative dose protocol: potential for improvements in reliability. *Radiation Measurements* 37: 377-381.
2. Wang XL, Wintle AG, Adamiec G (2012) Improving the reliability of single-aliquot regenerative-dose dating using a new method of data analysis. *Quaternary Geochronology* 9: 65-74.

3. Galbraith RF, Roberts RG, Laslett GM, Yoshida H, Olley JM (1999) Optical dating of single and multiple grains of quartz from jinmium rock shelter, northern Australia, part 1, Experimental design and statistical models. *Archaeometry* 41: 339-364.
4. Galbraith RF, Roberts RG (2012) Statistical aspects of equivalent dose and error calculation and display in OSL dating: An overview and some recommendations. *Quaternary Geochronology* 11: 1-27.
5. Wang XL, Wintle AG (2012) Optically stimulated luminescence production in the single-aliquot regenerative dose protocol. *Radiation Measurements* 47: 121-129.
6. Mejdahl V, Christiansen HH (1994) Procedures used for luminescence dating of sediments. *Boreas* 13: 403-406.
7. Duller GAT, Bøtter-Jensen L, Murray AS (2003) Combining infrared and green-laser stimulation sources in single-grain luminescence measurements of feldspar and quartz. *Radiation Measurements* 37: 543-550.
8. Olley JM, Pietsch T, Roberts RG (2004) Optical dating of Holocene sediments from a variety of geomorphic settings using single grains of quartz. *Geomorphology* 60: 337-358.
9. Wright DK, Forman SL, Waters MR, Ravesloot JC (2011) Holocene eolian activation as a proxy for broad-scale landscape change on the Gila River Indian Community, Arizona. *Quaternary Research* 76: 10-21.
10. Fain J, et al. (1999) Luminescence and ESR dating-Beta-dose attenuation for various grain shapes calculated by a Monte-Carlo method. *Quaternary Science Reviews* 18: 231-234.
11. Prescott JR, Hutton JT (1994) Cosmic ray contributions to dose rates for luminescence and ESR dating: large depths and long-term time variations. *Radiation Measurements* 23: 497-500.
12. Guerin G, Mercier N, Adamiec G (2011) Dose-rate conversion factors: update. *Ancient TL* 29: 5-8.
13. Kaufman S Libby WF (1954) The natural distribution of tritium. *Phy. Rev*. 93: 1337-1344.

14. Baeza A, García E, Miró C (1999) A procedure for the determination of very low activity levels of tritium in water samples. *Journal of Radioanlytical and Nuclear Chemistry* 241: 93-100.